Study of Magnetoconvection Impact on a Coil Cooling by Ferrofluid with a Spectral/Finite-Element Method

Raphaël Zanella[1,2,3], Caroline Nore[1], Frédéric Bouillault[2], Loïc Cappanera[3], Ignacio Tomas[3], Xavier Mininger[2], and Jean-Luc Guermond[3]

[1]LIMSI, CNRS, Université Paris-Sud, Université Paris-Saclay, F-91405 Orsay, France
[2]GeePs, UMR 8507 CNRS/CentraleSupelec—Universités UPMC et UPSud, 91192 Gif sur Yvette cedex, France
[3]Department of Mathematics, Texas A&M University, College Station, TX 77843 USA

The benefit of magnetoconvection for transformer cooling by ferrofluid is numerically studied. A code combining spectral and finite-element methods is applied on a solenoid system. Magnetostatic, Navier–Stokes, and energy equations are solved simultaneously. A vegetable oil seeded with magnetite nanoparticles at a volume fraction of 10% is considered. The magnetization of the ferrofluid is a function of temperature through an approximation of the classical Langevin's law. Magnetic and temperature fields are used to update the magnetic action, modeled by the Kelvin force, on the ferrofluid momentum at each time step. Numerical results for regular oil are consistent with experimental temperature data obtained for pure vegetable oil cooling. Numerical results for ferrofluid show that the magnetoconvection modifies the flow convection pattern and speed. The temperature increase in the coil is consequently reduced by about 9.4% with ferrofluid cooling.

Index Terms— **Coupled problem, finite element, magnetoconvection, spectral method, transformer cooling.**

I. Introduction

A FERROFLUID is a stable suspension of magnetic nanoparticles in a non-magnetic liquid carrier. A magnetic field transfers momentum to the ferrofluid through the nanoparticles. Literature often mentions the Kelvin force model (in N/m^3) to consider this effect [1]

$$\boldsymbol{F} = \mu_0(\boldsymbol{M} \cdot \nabla)\boldsymbol{H} \tag{1}$$

where $\boldsymbol{M}$ is the magnetization and $\boldsymbol{H}$ is the magnetic field.

The dependence of the magnetization with respect to temperature can lead to magnetoconvection when magnetic field and temperature gradients are combined, as it is the case in immersed transformers [2]. If the heat transfer rate is increased because of the nanoparticles, then the volume of cooling fluid could be reduced, or mechanical cooling systems could be avoided. Moreover, instead of conventional mineral oil, the liquid carrier could be substituted by vegetable oil, with higher viscosity but biodegradable and non-toxic.

Heat transfer enhancement, when using ferrofluid instead of regular oil, was pointed out in the work on an immersed coil [3]. Encouraging results on a transformer were obtained in [4], but the ferrofluid magnetization model was temperature independent. The experimental work based on a transformer prototype [5] also showed the benefit of ferrofluid as coolant. In this paper, a setup close to that of [3] is simulated with the SFEMaNS code [6], based on spectral and finite-element methods. The ferrofluid magnetization follows an approximation of Langevin's law [7] to include the effects of temperature dependence. Dynamics and symmetry features of the solutions, with or without nanoparticles, are presented, and the decrease of the coil temperature with ferrofluid cooling is explained by studying the flow pattern.

In the first step, a simulation without Kelvin force is ran to validate the model against an experiment with pure vegetable oil. In the second step, the Kelvin force is added and the numerical results for regular oil and ferrofluid are compared.

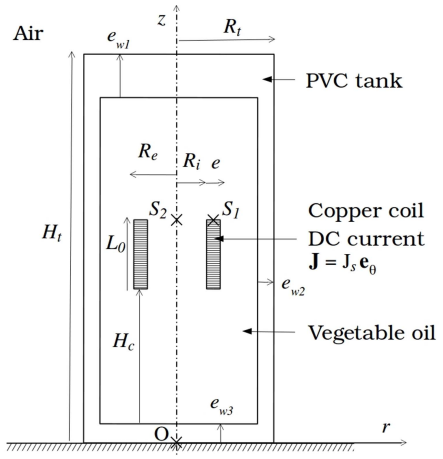

Fig. 1. Experimental setup model. S_1 and S_2 represent the thermal sensors.

II. Experimental Setup and Modeling

A. Experimental Setup

The experiment [8] is based on an electromagnetic system constituted of a triple copper coil crossed by a dc current and immersed in vegetable oil, as presented in Fig. 1. The fluid is a sample of oil produced by the Midel company for transformer cooling. The temperature increase is locally measured at the boundary of the coil and in the fluid until a steady state is reached (typically 10 000 s time).

The dimensions are $H_t = 12.5$ cm, $R_t = 2.5$ cm, $R_i = 0.8$ cm, $R_e = 1.175$ cm, $e = 0.375$ cm, $L_0 = 2.1$ cm, $H_c = 3.9$ cm, $e_{w1} = 2$ cm, $e_{w2} = 0.45$ cm, and $e_{w3} = 1$ cm.

Manuscript received June 26, 2017; accepted August 29, 2017. Date of publication September 6, 2017; date of current version February 21, 2018. Corresponding author: R. Zanella (e-mail: zanella@limsi.fr).

Color versions of one or more of the figures in this paper are available online at http://ieeexplore.ieee.org.

Digital Object Identifier 10.1109/TMAG.2017.2749539

The current in each spire, about 8 A, is controlled with a dSPACE setup so that the power dissipated in the coil keeps its initial value of 3 W over the period of measurement. The coil electrical resistance decrease due to the heating by Joule effect is thus counterbalanced.

B. Modeling

Regular oil and ferrofluid cases use the same equations, except for the body forces in the momentum equation, as presented hereafter. Quasi-steady regime approximation for electromagnetism is used. Like the regular oil, the ferrofluid is a continuum medium with Newtonian fluid behavior [1]. Boussinesq approximation is used and viscous dissipation is neglected. Regarding the ferrofluid, its magnetization is assumed to be instantaneously aligned with the magnetic field.

The magnetostatic equations are

$$\nabla \times \boldsymbol{H} = \boldsymbol{J} \tag{2}$$

$$\nabla \cdot (\mu \boldsymbol{H}) = 0 \tag{3}$$

where $\boldsymbol{J}$ is the current density (enforced current density $J_s \boldsymbol{e}_\theta$ in the coil, null elsewhere) and μ is the magnetic permeability. The fluid equations, based on Navier–Stokes equations, are

$$\rho \partial_t \boldsymbol{u} + \rho(\boldsymbol{u} \cdot \nabla)\boldsymbol{u} + \nabla p - \eta \Delta \boldsymbol{u} = \alpha(T - T_0)\rho g \boldsymbol{e}_z + \mu_0 M \nabla H \tag{4}$$

$$\nabla \cdot \boldsymbol{u} = 0 \tag{5}$$

where ρ is the density, $\boldsymbol{u}$ is the velocity, p is the pressure, η is the dynamic viscosity, α is the thermal expansion coefficient, T is the temperature, T_0 is the exterior temperature, and g is the gravity. The first term of the right-hand side is the Boussinesq force and the second term represents the simplified expression of the Kelvin force in (1) considering that $\boldsymbol{M}$ and $\boldsymbol{H}$ are collinear [1]. The conservation of energy is written as

$$\rho c \partial_t T + \rho c(\boldsymbol{u} \cdot \nabla)T - \nabla \cdot (\lambda \nabla T) = f_T \tag{6}$$

where c is the heat capacity, λ is the thermal conductivity, and f_T is the heat source, equal to the Joule effect J_s^2/σ_{cl} in the coil and null elsewhere (σ_{cl} is the coil electrical conductivity). The magnetic field impacts the velocity with no retroaction. Velocity and temperature are strongly coupled and are thus solved simulteneously.

The boundary condition $\boldsymbol{H} \times \boldsymbol{n} = 0$ is applied on the tank's exterior border. The non-slip boundary condition $\boldsymbol{u} = 0$ is enforced on the border of the fluid domain. The air convection at the top and the lateral boundaries of the tank are modeled by a Robin boundary condition on temperature

$$-\lambda \nabla T \cdot \boldsymbol{n} = h(T - T_0) \tag{7}$$

where h is the convection coefficient and $\boldsymbol{n}$ is the outer normal vector. The Dirichlet condition $T = T_0$ is enforced on the bottom of the tank, which is in contact with the setup table. Initially, $\boldsymbol{u} = 0$, $T = T_0$, and $\boldsymbol{H} = 0$.

The magnetization intensity of the ferrofluid is proportional to the magnetic field intensity

$$M = \chi(T)H \tag{8}$$

with χ the susceptibility given by an approximation of Langevin's law [7]

$$\chi(T) = \frac{\varphi \mu_0 \pi d^3 M_0^2}{18 k_B (T + 273.15)} \tag{9}$$

where φ is the volume fraction of magnetic material, d is the particle diameter, M_0 is the particle magnetization and k_B is Boltzmann's constant.

TABLE I
THERMOPHYSICAL PROPERTIES

Property	Coil	Fluid	Tank
Density (kg/m^3)	3888	922	1400
Dynamic viscosity (Pa·s)	-	2.9e-2	-
Thermal expansion coefficient (/K)	-	7.4e-4	-
Heat capacity (J/K·kg)	622	1970	1000
Thermal conductivity (W/m·K)	0.361	0.166	0.16

The thermophysical properties used in each subdomain (coil, fluid, tank) are presented in Table I.

The viscosity is set to the value taken at 40 °C, the temperature approximately reached at the end of the experiment. The other fluid properties present reduced variations over the temperature range and are taken at 20 °C.

In the model, the coil represents the copper coil itself and the oil stuck by viscosity between the spires. The properties are homogeneous between copper and Midel oil properties, the volume fraction of copper being approximately 37%. The density and the heat capacity are obtained by using a mix law. The thermal conductivity is given by the analytical law developped in [9].

The temperature in the lab is measured at $T_0 = 18$ °C. The tank/air convection coefficient is chosen in the range given by the literature: $h = 17$ W/m$^2 \cdot$ K. The Joule effect and the current density in the coil are calculated to be consistent with the enforced current in the experiment.

A ferrofluid containing magnetite nanoparticules with classical characteristics is considered: $\varphi = 0.1$, $d = 10$ nm, and $M_0 = 446$ kA/m. In the magnetostatic equation (3), the magnetic permeability μ is piecewise constant: $\mu_0(1 + \chi(T_0))$ in the ferrofluid and μ_0 is elsewhere.

III. SFEMaNS Code

A. Numerical Method

We use our own magnetohydrodynamics code called SFEMaNS (see [6]), using a hybrid spatial discretization mixing Fourier expansions and finite elements. The method is based on cylindrical coordinates, and every field f is solved as a partial Fourier sum relative to the azimuthal direction

$$f(r, \theta, z) = f_0^c(r, z) + \sum_{m=1}^{m_{\max}} f_m^c(r, z) \cos(m\theta) + \sum_{m=1}^{m_{\max}} f_m^s(r, z) \sin(m\theta) \tag{10}$$

where $m_{\max}$ is the maximum considered mode. The problem can be approximated independently (modulo the computations of nonlinear terms) for each Fourier mode in the meridian plane with Lagrange finite elements. Thanks to the Fourier decomposition, SFEMaNS can be less computationally expensive than a classical 3-D finite-element code on axisymmetric geometries. Second-order elements are used for the temperature and the velocity, while first-order elements are used for the pressure for computational efficiency. For the magnetic part, the algorithm solves the problem using the magnetic field $\boldsymbol{H}$ in the conducting region (after standard elimination of

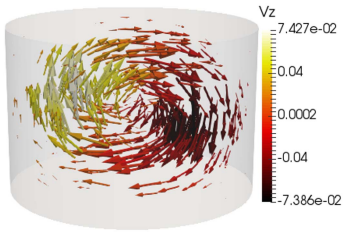

Fig. 2. Rayleigh–Bénard convection roll [13] simulated by SFEMaNS.

the electric field) and a scalar magnetic potential ($\boldsymbol{H} = \nabla\phi$) in the insulating exterior if needed. The fields in each region are approximated by using H^1-conforming Lagrange elements, with a technique to enforce $\nabla \cdot (\mu \boldsymbol{H}) = 0$ based on a penalty method. The coupling across the axisymmetric interfaces of discontinuous electric conductivity or magnetic permeability is enforced by an interior penalty method. The equations are solved separately at each time step, allowing strong couplings.

SFEMaNS has been thoroughly validated on numerous analytical solutions and against other magnetohydrodynamics codes [6], [10]–[12].

B. Validation on a Rayleigh–Bénard Convection Test Case

We study a classical Rayleigh–Bénard convection problem in a cylindrical cavity heated from below and insulated laterally following [13]. Using non-slip boundary conditions on the lateral wall, the motionless conducting state of a cylinder of radius to height aspect ratio of $R/H = 0.75$ becomes unstable above a critical Rayleigh number

$$Ra = \frac{\alpha \Delta T g H^3}{\kappa \nu} = 2590 \tag{11}$$

where ΔT is the characteristic temperature difference, κ is the thermal diffusivity, and ν is the kinematic viscosity, in excellent agreement with [13]. The stationary convection forms a roll corresponding to a $m = 1$ mode, which breaks the axisymmetry of the base state (see Fig. 2).

IV. Results

A. Comparison With the Experiment on Pure Vegetable Oil

The flow and temperature fields are simulated in the experiment case of pure vegetable oil. In (4), the only force is the Boussinesq one, and (2) and (3) are not solved.

Computations show that, for the chosen parameters, the steady solution is carried only by the mode 0, i.e., it is axisymmetric. Even initially populated, the other modes vanish and $m_{\max} = 0$ in (10) is chosen. The mesh contains 3031 nodes and a time step of 0.02 s is used over 5×10^5 iterations (about 11 wall-clock hours using eight processors on the cluster IBM x3750-M4 from GENCI-IDRIS).

The numerical solution reaches a steady regime in about 10 000 s, a time consistent with the experimental observation. Fig. 3 presents the time evolution of the kinetic energy

$$E_k(t) = \int_{\Omega f} \frac{1}{2} \rho u^2(\boldsymbol{x}, t) d\boldsymbol{x} \tag{12}$$

where Ω_f is the fluid domain, and the spatial quadratic mean of the temperature increment

$$\overline{T - T_0}\,(t) = \sqrt{\frac{1}{V} \int_{\Omega} (T - T_0)^2 (\boldsymbol{x}, t)\, d\boldsymbol{x}} \tag{13}$$

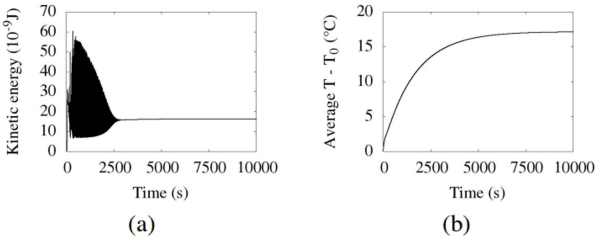

Fig. 3. (a) Time evolution of the kinetic energy and the (b) spatial quadratic mean of the temperature increment $T - T_0$ in the regular oil case.

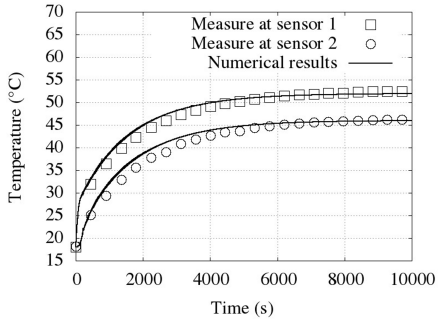

Fig. 4. Comparison of the temperature increase obtained experimentally and numerically in the pure vegetable oil case. Experimental data from [8].

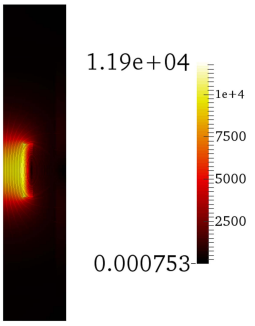

Fig. 5. Magnetic field intensity H (A/m) and field lines in a meridian plane (symmetry axis on the left) in the ferrofluid case.

where Ω is the whole domain and V is its volume. These global quantities show that velocity and temperature fields eventually reach a stationary state.

The numerical results for temperature are in good agreement with the experimental data, as shown in Fig. 4.

B. Numerical Results on Magnetoconvection

The code is used to assess the effect of the magnetoconvection when the vegetable oil is replaced by ferrofluid. Both Boussinesq and Kelvin forces create momentum in (4). In these simulations, the regular oil and the ferrofluid have the same thermophysical properties to highlight the Kelvin force effect.

The final solution is axisymmetric and $m_{\max} = 0$ is taken. The same numerical setup (mesh, time step, processors) leads to a completed computation in about 16 wall-clock hours.

The Kelvin force, generated by the magnetic field of Fig. 5, impacts the system dynamics. In this case, the velocity field does not reach a static state, as shown in Fig. 6(a). The kinetic energy, after an initial transitory regime, reaches a plateau and then switches (between 8000 and 9000 s) to an oscillating

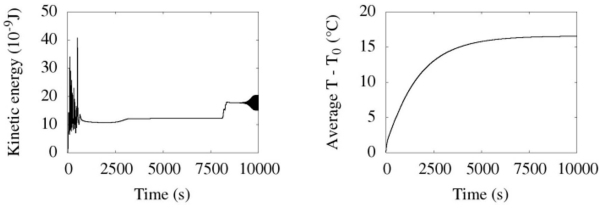

Fig. 6. (a) Time evolution of the kinetic energy and the (b) spatial quadratic mean of the temperature increment $T - T_0$ in the ferrofluid case.

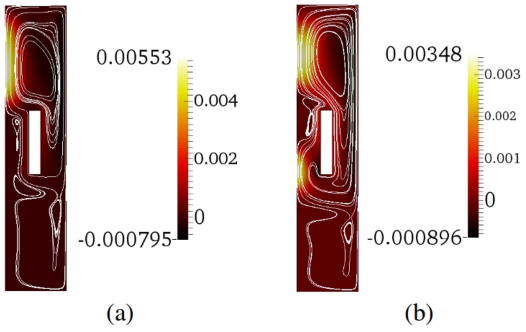

Fig. 7. Axial velocity u_z (m/s) and streamlines in a meridian plane (symmetry axis on the left) at $t = 10\,000$ s for (a) regular oil and (b) ferrofluid.

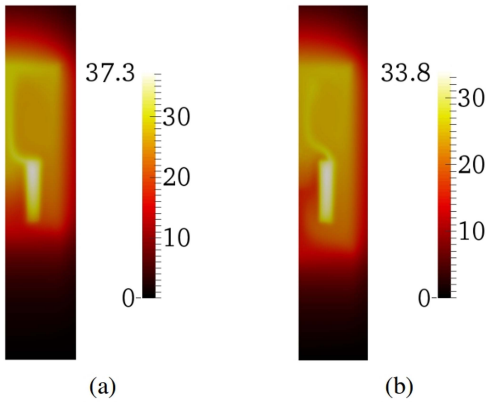

Fig. 8. Temperature increment $T - T_0$ (°C) in a meridian plane (symmetry axis on the left) at $t = 10\,000$ s for (a) regular oil and (b) ferrofluid.

state. Further computations show that the oscillations of the kinetic energy survive after $t = 10\,000$ s. The temperature field reaches an almost static state, oscillations due to the changes in the velocity field being very small, in the time needed for vegetable oil [Fig. 6(b)]. The cooling performance of ferrofluid can be assessed since the coil temperature is stable.

The flow pattern is transformed because of the Kelvin force. In the pure vegetable oil case [Fig. 7(a)], a natural convection cell appears at the top of the coil. The fluid flows up along the coil while heating and then flows down along the tank while cooling. In the ferrofluid case [Fig. 7(b)], a strong upward flow appears at the symmetry axis and leads to an additional convection cell that cools down the coil.

The magnetoconvection improves the heat removal in the ferrofluid system. The temperature increment $T - T_0$ in the coil goes from 37.3 °C with regular oil to 33.8 °C with ferrofluid (see Fig. 8). Thanks to the nanoparticles, the increase of temperature in the coil is reduced by about 9.4%.

V. Conclusion

A mathematical model has been developed to study transformer cooling with ferrofluid on an immersed coil case. The action of the magnetic field on the fluid is modeled by the Kelvin force while the magnetization of the ferrofluid follows Langevin's law for paramagnetism.

Numerical simulations based on an experimental setup are consistent with the temperature measured in the case of regular oil cooling. Numerical experiments show an improvement of the heat removal when regular oil is replaced by ferrofluid; the temperature rise in the coil being reduced by 9.4% due to magnetoconvection.

Further developments will include a model taking into account the modification of the fluid properties with nanoparticles and the comparison with ferrofluid experimental results.

Acknowledgment

This work was supported by the Labex LaSIPS (Nano-in-Oil Grant). Code's development and simulations were performed with HPC resources from TAMU and GENCI-IDRIS under Grant 2016-0254.

References

[1] J. L. Neuringer and R. E. Rosensweig, "Ferrohydrodynamics," *Phys. Fluids*, vol. 7, no. 12, pp. 1927–1937, Dec. 1964.
[2] S. Odenbach, *Magnetoviscous Effects in Ferrofluids* (Lecture Notes in Physics Monographs), vol. 71. Berlin, Germany: Springer, 2002.
[3] G.-Y. Jeong, S. P. Jang, H.-Y. Lee, J.-C. Lee, S. Choi, and S.-H. Lee, "Magnetic-thermal-fluidic analysis for cooling performance of magnetic nanofluids comparing with transformer oil and air by using fully coupled finite element method," *IEEE Trans. Magn.*, vol. 49, no. 5, pp. 1865–1868, May 2013.
[4] L. Pîslaru-Danescu, A. M. Morega, G. Telipan, M. Morega, J. B. Dumitru, and V. Marinescu, "Magnetic nanofluid applications in electrical engineering," *IEEE Trans. Magn.*, vol. 49, no. 11, pp. 5489–5497, Nov. 2013.
[5] J. Patel, K. Parekh, and R. V. Upadhyay, "Prevention of hot spot temperature in a distribution transformer using magnetic fluid as a coolant," *Int. J. Thermal Sci.*, vol. 103, pp. 35–40, May 2016.
[6] J.-L. Guermond, R. Laguerre, J. Léorat, and C. Nore, "Nonlinear magnetohydrodynamics in axisymmetric heterogeneous domains using a Fourier/finite element technique and an interior penalty method," *J. Comput. Phys.*, vol. 228, pp. 2739–2757, 2009.
[7] R. E. Rosensweig, "Magnetic fluids," *Annu. Rev. Fluid Mech.*, vol. 19, pp. 437–461, Jan. 1987.
[8] N. Puigmal, A. N. Djoudi, E. Berthelot, R. Zanella, and X. Mininger, "Etudes numériques et expérimentales du refroidissement par bain d'huile d'un système électromagnétique," in *Proc. NUMELEC Conf.*, Paris, France, Nov. 2017.
[9] W. T. Perrins, D. R. McKenzie, and R. C. McPhedran, "Transport properties of regular arrays of cylinders," *Proc. R. Soc. Lond. A, Math., Phys. Eng. Sci.*, vol. 369, no. 1737, pp. 207–225, 1979.
[10] A. Bonito, J.-L. Guermond, and F. Luddens, "Regularity of the Maxwell equations in heterogeneous media and Lipschitz domains," *J. Math. Anal. Appl.*, vol. 408, no. 2, pp. 498–512, 2013.
[11] C. Nore, H. Zaidi, F. Bouillault, A. Bossavit, and J.-L. Guermond, "Approximation of the time-dependent induction equation with advection using Whitney elements: Application to dynamo action," *COMPEL-Int. J. Comput. Math. Elect. Electron. Eng.*, vol. 35, no. 1, pp. 326–338, 2016.
[12] A. Giesecke *et al.*, "Influence of high-permeability discs in an axisymmetric model of the Cadarache dynamo experiment," *New J. Phys.*, vol. 14, no. 5, p. 053005, 2012.
[13] M. Wanschura, H. C. Kuhlmann, and H. J. Rath, "Three-dimensional instability of axisymmetric buoyant convection in cylinders heated from below," *J. Fluid Mech.*, vol. 326, pp. 399–415, Nov. 1996.